

# Particle decay in the early universe: predictions for 21 cm

Yu. A. Shchekinov<sup>1\*</sup> and E. O. Vasiliev<sup>2,3†</sup>

<sup>1</sup>*Department of Physics, University of Rostov, Sorge St. 5, Rostov-on-Don, 344090 Russia*

<sup>2</sup>*Tartu Observatory, 61602 Tõrvavere, Estonia*

<sup>3</sup>*Institute of Physics, University of Rostov, Stachki Ave. 194, Rostov-on-Don, 344090 Russia*

Accepted 2006 December 15. Received 2006 April 1; in original form 2006 April 1

## ABSTRACT

The influence of ultra-high energy cosmic rays (UHECRs) and decaying dark matter particles on the emission and absorption characteristics of neutral hydrogen in 21 cm at redshifts  $z = 10 - 50$  is considered. In presence of UHECRs 21 cm can be seen in absorption with the brightness temperature  $T_b = -(5 \div 10)$  mK in the range  $z = 10 - 30$ . Decaying particles can stimulate a 21 cm signal in emission with  $T_b \sim 50 - 60$  mK at  $z = 50$ , and  $T_b \simeq 10$  mK at  $z \sim 20$ . Observational possibilities to detect manifestations of UHECRs and/or decaying particles in 21 cm with the future radio telescopes (LOFAR, PAST and SKA), and to distinguish contributions from them are briefly discussed.

**Key words:** early Universe – cosmology:theory – dark matter – diffuse radiation.

## 1 INTRODUCTION

At  $z \sim 1000$  the universe enters the “dark ages” epoch, the electrons and protons recombine, and gas remains neutral until the first luminous objects emerge at  $z \sim 30 - 20$ . Neutral gas can be observed in a redshifted 21 cm line of neutral hydrogen in emission or absorption against the cosmic microwave background (CMB). This gives a possibility for studying the processes associated with transition of the neutral universe into a fully ionized state, and for identification of the sources responsible for reionization (Hogan & Rees 1979, Madau et al 1997). At present observations of 21 cm line are anticipated as a promising tool for diagnostics of the universe in the end of “dark ages” (Madau et al 1997, Tozzi et al 2000, Ciardi & Madau 2003).

Two possible sources of photons can be important for reionization: the baryons processed in stellar nucleosynthesis (Shapiro & Giroux 1987, Miralda-Escudé & Rees 1994, Tegmark et al 1994, Cen 2003, Ciardi et al 2003, Choudhury & Ferrara 2006) and/or in shock waves near black holes (Madau et al 1999, Oh 2001, Ricotti & Ostriker 2004), and ultra-high energy cosmic rays (Doroshkevich & Naselsky 2002) and unstable particles (Sciama 1982, Scott et al 1991). The first luminous objects are commonly thought to be the principal source of the reionization. They heat gas in the universe through ionization by ultraviolet (UV) and X-ray photons. This inevitably affects the emissivity of gas in the 21 cm line, because the hydrogen spin temperature  $T_s$  depends on the gas kinetic temperature  $T_k$ , and thus ob-

served intensity imprints the effects from the objects of the first generation (Madau et al 1997, Tozzi et al 2000, Ciardi & Madau 2003, Loeb & Zaldarriaga 2004, Zaldarriaga et al 2004, Chen & Miralda-Escudé 2004, Sethi 2005).

Production of copious number of ionizing photons during the dark ages can be connected with the origin of ultra-high energy cosmic ray (UHECRs) if they form from decaying superheavy dark matter (SHDM) particles with masses  $M_X \gtrsim 10^{12}$  GeV in the so-called top-to-bottom scenario (Berezinsky et al 1997, Kuzmin & Rubakov, 1998, Birkel & Sarkar, 1998). The associated production of UV photons can have strong influence on cosmological recombination (Doroshkevich & Naselsky 2002, Doroshkevich et al 2003).

Decaying dark matter particles, such as massive neutrinos, can also contribute significantly to reionization (Sciama 1982, Dodelson & Jubas 1994). Polarisation measurements of the CMB by the Wilkinson Microwave Anisotropy Probe (WMAP) satellite (Spergel et al 2003) imparted a new impulse to this possibility. The obtained relatively large optical depth of the universe  $\tau \simeq 0.16$  suggests unrealistically strong constraints on properties of the first stellar objects (e.g. Cen 2003, Wyithe & Loeb 2003, see also an alternative discussion in Tumlinson et al 2004), which lead to assume that decaying dark matter can be at least a complementary source of reionization (Hansen & Haiman 2004, Chen & Kamionkowski 2004 (CK), Kasuya et al 2004, Kasuya & Kawasaki 2004, Pierpaoli 2004, Mapelli et al 2006). The corresponding heating can change characteristics of 21 cm in emission and absorption.

In this paper we study the effects from UHECRs and decaying particles on cosmological 21 cm background. We assume a  $\Lambda$ CDM cosmology with the parameters

\* E-mail:yus@phys.rsu.ru

† E-mail:eugstar@mail.ru

$(\Omega_0, \Omega_\Lambda, \Omega_m, \Omega_b, h) = (1.0, 0.76, 0.24, 0.041, 0.73)$  (Spergel et al 2006).

## 2 SPIN TEMPERATURE

The two processes: atomic collisions and scattering of UV photons, couple the HI spin temperature and the gas kinetic temperature (Field 1958)

$$T_s = \frac{T_{CMB} + y_a T_k + y_c T_k}{1 + y_a + y_c} \quad (1)$$

here  $T_{CMB}$  is the CMB temperature,  $y_c, y_a$  are the functions determined by the collisional excitations and the intensity of the UV resonant photons

$$y_a = \frac{P_{10} T_*}{A_{10} T_k}, \quad y_c = \frac{C_{10} T_*}{A_{10} T_k} \quad (2)$$

$T_*$  = 0.0682 K is the hyperfine energy splitting,  $A_{10} = 2.87 \times 10^{-15} \text{ s}^{-1}$  is the spontaneous emission rate of the hyperfine transition,  $C_{10} = k_{10} n_H + \gamma_e n_e$  is the collisional de-excitation rate by hydrogen atoms and electrons, the rate by protons is negligible, for  $k_{10}$  we use the approximation by Kuhlen et al (2005), for  $\gamma_e$  we take the approximation from Liszt (2001),  $P_{10}$  is the indirect de-excitation rate, which is related to the total Ly $\alpha$  scattering rate  $P_a$  (Field 1958)

$$P_{10} = 4P_a/27, \quad (3)$$

where

$$P_a = \int c n_\nu \sigma_\nu d\nu \quad (4)$$

$n_\nu$  is the number density of photons per unit frequency range,  $\sigma(\nu)$  is the cross section for Ly $\alpha$  scattering (Madau et al 1997). The brightness temperature in 21 cm is then (Field 1958, Chen & Miralda-Escudé 2004)

$$T_b = 25 \text{ mK} \left( \frac{T_s - T_{CMB}}{T_s} \right) \left( \frac{\Omega_b h_0}{0.03} \right) \left( \frac{0.3}{\Omega_m} \right)^{1/2} \left( \frac{1+z}{10} \right)^{1/2} \quad (5)$$

## 3 IONIZATION AND THERMAL HISTORY OF THE UNIVERSE

Evolution of the fractional ionization is described by

$$\frac{dx_e}{dz} = \frac{1}{(1+z)H(z)} (R_s(z) - I_s(z) - I_e(z)) \quad (6)$$

where besides the standard recombination and ionization rates  $R_s(z), I_s(z)$ , the term  $I_e(z)$  is explicitly introduced due to presence of additional sources of UV photons. For the UHECRs this term can be written in the form (Peebles et al 2000, Doroshkevich & Naselsky 2002)

$$I_e(z) = \epsilon(z) H(z) x_H, \quad (7)$$

where  $\epsilon(z) = \epsilon_0/(1+z)$  is the production of ionizing photons,  $H(z)$  is the Hubble parameter,  $x_H$  is the fraction of neutral hydrogen. For decaying particles this term is written as (CK)

$$I_e(z) = \chi_i f_x \Gamma_X \frac{m_p c^2}{h \nu_c} \quad (8)$$

where  $\chi_i$  is the energy fraction deposited into ionization for which we made use the calculations by Shull & van Steenberg (1985),  $m_p$  is the proton mass,  $f_x = \Omega_X(z)/\Omega_b(z)$ ,  $\Omega_b(z)$  is the baryon density parameter,  $\Omega_X(z)$  is the fractional abundance of decaying particles,  $\Gamma_X$  is the decay rate,  $h \nu_c$  is the energy of Ly-c photons. For short living particles  $\Omega_X(z) \propto e^{-\Gamma_X t}$  and their contribution to ionization and heating essentially vanishes at  $t > \Gamma_X^{-1}$ ; normally  $\Gamma_X^{-1}$  is assumed to be comparable to the comoving Hubble time in the range of redshifts of interest.

The gas temperature is determined by equation

$$(1+z) \frac{dT}{dz} = 2T + k_C \frac{x_e}{H(z)(1+f_{He}+x_e)} (T - T_{CMB}) \quad (9)$$

$$- \frac{2}{3k} \frac{K}{H(z)(1+f_{He}+x_e)}$$

where the second term in the r.h.s. describes the energy exchange between the gas and CMB photons  $k_C = 4.91 \times 10^{-22} T_{CMB}^4$ ,  $f_{He} = 0.24$ , the third term is the heating from additional sources of the ionizing photons,  $K$  is the corresponding heating rate which can be written in the form (CK)

$$K = \chi_h m_p c^2 f_x \Gamma_X \quad (10)$$

where  $\chi_h$  is the energy fraction depositing into heating; as for  $\chi_i$  we used for  $\chi_h$  the results of Shull & van Steenberg (1985). By order of magnitude  $\chi_i \sim \chi_h \sim 1/3$  for the conditions we are interested in.

In the presence of UHECRs the final products are only Ly $\alpha$  and Ly-c photons (Doroshkevich & Naselsky 2002). As pointed out by (Chen & Miralda-Escudé 2004) the injected Ly $\alpha$  photons change the gas temperature very little:  $K_\alpha = 0$ . Ly-c photons have the energy slightly in excess of the hydrogen binding energy:  $\sim 13.6 \text{ eV} + 3kT/2$ . Therefore the heating rate from the UHECRs produced Ly-c photons  $K_c$  has to be calculated self-consistently together with equation (10). However, as we will see later the gas kinetic temperature in presence of UHECRs is at most 150 K, so that the heating rate from Ly-c photons is always less than  $\sim 2 \times 10^{-31} \epsilon (1+z)^{3/2} \text{ erg cm}^{-3} \text{ s}^{-1}$ . The corresponding contribution to the gas kinetic temperature is less than a few percent.

We apply a modified version of the code RECFAST (Seager et al 1999) to solve equations (6), (10).

## 4 RESULTS

Stellar and quasi-stellar sources of ionizing radiation begin to form at redshifts  $z < 20$ , and gas around them heated through photoionization can emit in 21 cm with a spot-like distribution. The spots have too small angular sizes, and can be detected only later, when at  $z \lesssim 15$  star formation increases and forms pervading domains of sufficiently hot gas (Zaroubi & Silk 2004). Instead, UV photons from additional ionizing sources, like UHECRs and decaying particles, illuminate and heat the IGM homogeneously, and therefore the signal from 21 cm can be more easily detected from the earliest redshifts.

Fig. 1 shows kinetic and spin temperatures for a selected set of ionizing photon production rates by UHECRs and

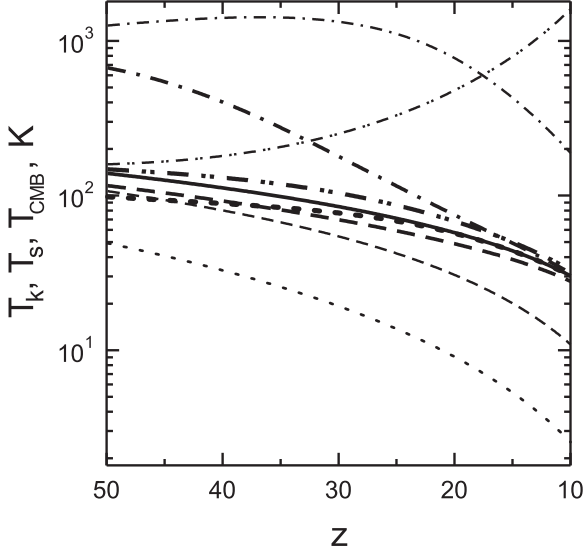


**Figure 1.** The kinetic (thin lines), spin (thick lines) and CMB (thick solid line) temperatures for the standard recombination  $\epsilon = 0$  (dotted), in the presence of UHECRs for the UV production rate  $\epsilon = 1$  (dashed), and in the presence of decaying particles: long living with  $\xi = 3 \times 10^{-26} \text{ s}^{-1}$  (dot-dot dashed), and short living with  $\Gamma_X = 10^{-15} \text{ s}^{-1}$ ,  $f_X(z_{eq}) = 10^{-8}$  (dash-dotted).

decaying particles. For the standard history ( $\epsilon = 0$ ) the spin temperature is nearly equal to the CMB value at  $z \leq 20$ , and the intergalactic gas cannot produce distinguishable signal in 21 cm in this redshift range. The kinetic temperature for UHECRs with  $\epsilon = 1$  is more than twice of the value in the standard ionization history ( $\epsilon = 0$ ). The increase of kinetic temperature for higher  $\epsilon$  is due to an increase of the fractional ionization of gas and a stronger coupling between the CMB photons and electrons. As a result, the gas kinetic temperature in this case shows similar variation with  $z$  as the CMB temperature. Due to collisional de-excitations of the hyperfine structure level this increase in  $T_k$  unavoidably results in a decrease of the spin temperature, such that the difference between the spin and CMB temperature in the range  $z \sim 35 - 10$  is for  $\epsilon = 1$  greater than for  $\epsilon = 0$ ;  $T_s - T_{CMB}$  vanishes at  $z \leq 10$ . This means that the signal in 21 cm can be detected in the redshift range  $z \sim 10 - 35$  in absorption. The long living particles provide a permanent heating the injection energy rate  $3k\dot{T}/2 = K/(1 + f_{He} + x_e)$ , such that for a sufficiently high heating (ionization) rate shown in Fig. 1 the gas kinetic temperature in this case grows towards lower  $z$  as seen in Fig. 1 (thin dot-dot dashed line). Contrary, the short living particles inject heat with the rate  $\dot{T} \propto e^{-\Gamma_X t}$ , which manifests in a relatively fast decrease of the kinetic temperature at low  $z$  (thin dash-dotted line in Fig. 1). The HI spin temperature remains in both cases above the CMB temperature.

Fig. 2 presents brightness temperature versus redshift for several values of  $\epsilon$ . An obvious qualitative difference between the standard model ( $\epsilon = 0$ ) and the models with  $\epsilon \geq 0.3$  is clearly seen: contrary to the standard case in

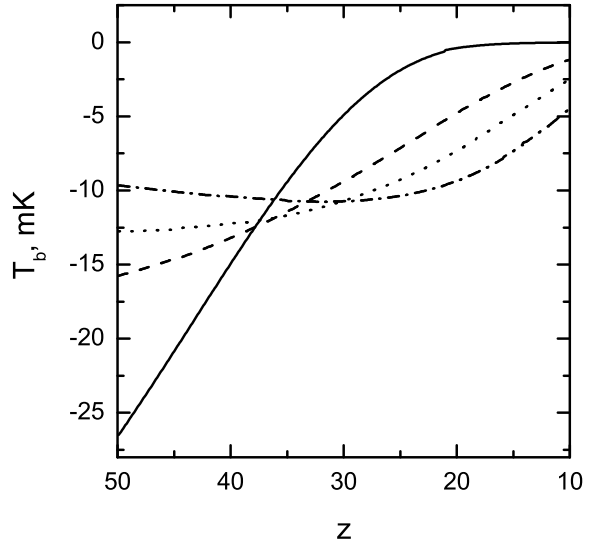


**Figure 2.** The brightness temperature in the presence of UHECRs for the UV production rate  $\epsilon = 0$  (solid),  $\epsilon = 0.3$  (dashed),  $\epsilon = 1$  (dotted),  $\epsilon = 3$  (dash-dotted).

all models  $T_b$  flattens at  $z > 30$  at the level  $T_b \simeq -(10 \div 15)$  mK. On the other hand at  $z < 25$ , where the standard model shows almost zero  $T_b$  all models with  $\epsilon \geq 0.3$  have brightness temperature between -5 and -10 mK. Thus, an 1000 hours LOFAR and/or SKA observation can discriminate between the standard and  $\epsilon \geq 0.3$  models.

Fig. 3a shows the brightness temperature for the long living decaying particles. The gas kinetic temperature grows with heating rate and can be lower or greater than  $T_{CMB}$  depending on  $\xi$ . Therefore, at low heating rate ( $\xi \leq 6 \times 10^{-27} \text{ s}^{-1}$ ) gas can be observed in 21 cm only in absorption, essentially approaching the standard case (compare the lower line in Fig. 3a with the solid line in Fig. 2). The transition from absorption to emission occurs at  $\xi \geq 10^{-26} \text{ s}^{-1}$ . Brightness temperature for short living particles is shown in Fig. 3b. In this case  $T_b$  increases with the heating rate similar to what occurs for the long living particles, and correspondingly at a sufficiently high heating 21 cm can be observed in emission. There is, however, a qualitative difference between the dependence of brightness temperature on redshift in these two cases: for the long living particles  $T_b(z)$  has always negative second derivative, while in the case of the short living particles  $T_b(z)$  has an inflection point. Note in this connection that  $T_b(z)$  curves in models with the UHECRs have always positive second derivative.

This circumstance may have a principal significance for choosing a strategy for observational discrimination between manifestations from the three sources of the ionizing photons, provided that observations are possible for a wide range of redshifts, from  $z = 10$  to  $z = 50$ . However, if the qualitative difference between  $T_b(z)$  curves for the UHECRs and long living particles seems to be relatively easily observationally distinguishable, it looks problematic for the curves  $T_b(z)$  in cases of the long and short living particles

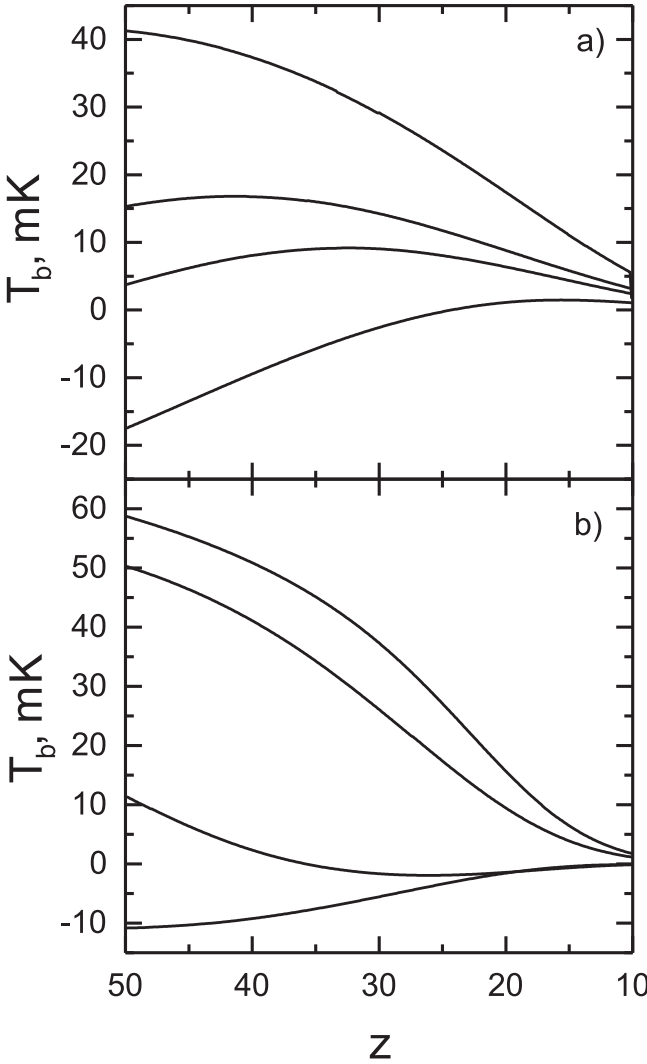


**Figure 3.** *Upper panel* – the brightness temperature in the presence of long living particles  $\Gamma_X \ll H_0$ :  $\xi = 6 \times 10^{-27} \text{ s}^{-1}$ ,  $3 \times 10^{-26} \text{ s}^{-1}$ ,  $6 \times 10^{-26} \text{ s}^{-1}$ ,  $3 \times 10^{-25} \text{ s}^{-1}$  – from the lowermost to the uppermost;  $\xi = \chi_i f_X \Gamma_X$ . *Lower panel* – the brightness temperature in the presence of short living particles  $\Gamma_X \gtrsim H_0$ :  $\Gamma_X = 10^{-14} \text{ s}^{-1}$ ,  $f_X(z_{eq}) = 0.5 \times 10^{-8}$ ,  $\Gamma_X = 5 \times 10^{-15} \text{ s}^{-1}$ ,  $f_X(z_{eq}) = 10^{-8}$ ,  $\Gamma_X = 10^{-15} \text{ s}^{-1}$ ,  $f_X(z_{eq}) = 10^{-8}$ ,  $\Gamma_X = 10^{-15} \text{ s}^{-1}$ ,  $f_X(z_{eq}) = 5 \times 10^{-8}$  – from the lowermost to the uppermost.

because the inflection of  $T_b(z)$  in the latter case lies within  $\Delta T_b(z) \simeq 5 \text{ mK}$ . From this point of view two-“color” diagrams, connecting the differences between the brightness temperatures at different wavelengths, can be complementary to the analysis of  $T_b(z)$  curves. We show an example of such two-“color” diagrams for the three sources of UV photons: UHECRs, long and short living decaying particles in Fig. 4. Specifically, we plot the temperature difference  $\Delta T_{23} = T_b(\lambda_2) - T_b(\lambda_3)$  versus  $\Delta T_{12} = T_b(\lambda_1) - T_b(\lambda_2)$ , where  $\lambda_1 = 210 \text{ cm}$ ,  $\lambda_2 = 420 \text{ cm}$ ,  $\lambda_3 = 840 \text{ cm}$  for a set of models for these three cases. The three cases fall into quite distinct regions in the two-“color” plane with a separation

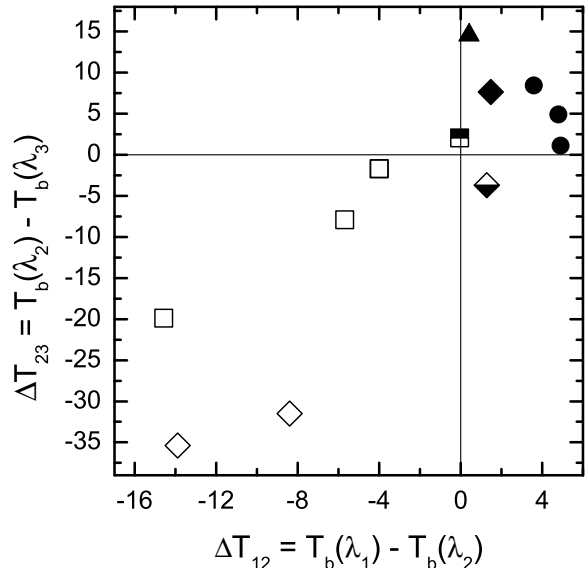


**Figure 4.** Two-“color” diagram for the models with UHECRs and decaying particles. Open symbols show differences in brightness temperatures in emission, filled – in absorption; half-filled correspond to emission at low  $z$  (lower half is open) and absorption at high  $z$  (upper half is filled), and vice versa. Circles show  $(\Delta T_{12}, \Delta T_{23})$  for UHECRs, diamonds – for long living decaying particles, squares – for short living particles, the triangle depicts the standard (no additional ionizing photons) case.

of  $\Delta T > 5 \text{ mK}$ , and thus can in principle be discriminated observationally.

The parameters of decaying particles and UHECRs we explored in this work are consistent with the current constraints. CK found using WMAP data  $\xi < 10^{-24} \text{ s}^{-1}$  for the long living particles, and a slightly weaker upper limit for the short living ones. Recent results from WMAP give a lower value of the optical depth  $\tau \lesssim 0.09$  (Spergel et al 2006). This strengthens the constraints on the parameters of decaying particles compared to those inferred from the WMAP data of the first year. However, as pointed out by CK decaying particles with short lifetimes do not affect significantly the optical depth and are thus less constrained. On the other hand, the upper limit for  $\xi = 3 \times 10^{-25} \text{ s}^{-1}$  for long living particles we consider here is within the range corresponding to the optical depth obtained from the third year WMAP data. For UHECRs Doroshkevich & Naselsky (2002) inferred from the MAXIMA-1 and BOOMERANG data (de Bernardis et al 2000, Hanany et al 2000)  $\epsilon \leq 3$ . Observations of HI at  $z = 10 - 50$  in 21 cm can provide further constraints. The sensitivity of ongoing long-wavelength experiments, such as LOFAR, PAST, MWA, LWA, SKA and LUDAR (Carilli 2006) seems to be sufficient to detect signal in 21 cm affected by decaying particles and UHECRs at pre-ionization epochs.

## 5 CONCLUSIONS

In this paper we have considered the influence of UV photons from decaying dark matter particles and UHECRs on the ability of neutral hydrogen to emit and/or absorb in 21 cm at redshifts  $z = 10 - 50$ . We have found that

- the three sources of additional ionizing photons: long living and short living unstable dark matter particles and UHECRs produce fairly distinct dependences of brightness temperature on redshift  $T_b(z)$  – the first and the third give negative and positive second derivatives of the curves  $T_b(z)$ , while the second has  $T_b(z)$  with an inflection point;
- three wave-band observations at  $\lambda_1$ ,  $\lambda_2$  and  $\lambda_3$  and a two-“color” diagram  $\Delta T_{23} = T_b(\lambda_2) - T_b(\lambda_3)$  versus  $\Delta T_{12} = T_b(\lambda_1) - T_b(\lambda_2)$  can provide an additional tool for discrimination between the sources of ionizing photons in the end of dark ages.

In general, decaying dark matter particles can have strong effects on overall history of the universe: they may change its thermal evolution and cosmological nucleosynthesis (Scherrer 1984, Vayner et al 1985, Kohri 2001, Kawasaki et al 2005), dynamics of large scale structure formation (Doroshkevich et al 1989, Bharadwaj & Sethi 1998, Cen 2001), reionization regime (Sciama 1982, Dodelson & Jubas 1994, Hansen & Haiman 2004, Chen & Kamionkowski 2004, Kasuya et al 2004, Kasuya & Kawasaki 2004, Pierpaoli 2004, Mapelli et al 2006). 21 cm emission from the epochs ending the dark ages can carry the imprints from decaying particles, and seems a promising tool for understanding their properties. Future radio telescopes (such as LOFAR, PAST, MWA, LWA and SKA) seem to have sufficient flux sensitivity for detection the signal in 21 cm influenced by decaying particles and UHECRs.

## 6 ACKNOWLEDGEMENTS

This work is supported by the Federal Agency of Education (project code RNP 2.1.1.3483) and by the RFBR (project code 06-02-16819-a).

## REFERENCES

Berezinsky, V.S., Kachelrieß, M. & Vilenkin, A., 1997, Phys. Rev. Lett., 79, 4302

Bharadwaj S., Sethi S., 1998, ApJS, 114, 37

Birkel, M. & Sarkar, S., 1998, Astropart. Phys., 9, 298

Carilli C.L., 2006, NewAR, 50, 162

Cen R., 2001, ApJL, 546, 77

Cen R., 2003, ApJL, 591, L5

Chen, X. & Kamionkowski, M., 2004, Phys. Rev. D, 70, 043502 (CK)

Chen X. & Miralda-Escudé J., 2004, ApJ, 602, 1

Ciardi B., Ferrara A., White S.D.M., 2003, MNRAS, 344, L7

Ciardi B. & Madau P., 2003, ApJ, 596, 1

Choudhury T.R. & Ferrara A., 2006, astro-ph/0603149

de Bernardis P. et al, 2000, Nature, 404, 955

Dodelson S., Jubas J.M., 1994, MNRAS, 266, 886

Doroshkevich A.G., Khlopov M.Yu. & Klypin A.A., 1989, MNRAS, 239, 923

Doroshkevich, A.G., Naselsky, I.P., Naselsky, P.D., Novikov, I.D., 2003, ApJ, 586, 709

Field G.B., 1958, Proc. IRE, 46, 240

Hanany S. et al, 2000, ApJ, 545L, 5

Hansen, S.H., & Haiman, Z., 2004, ApJ, 600, 26

Hogan C.J. & Rees M.J., 1979, MNRAS, 188, 791

Kasuya S. & Kawasaki M., 2004, Phys. Rev. D, 70, 103519

Kasuya S., Kawasaki M. & Sugiyama, N., 2004, Phys. Rev. D, 69b, 3512

Kawasaki M., Kohri K., Moroi T., 2005, Phys. Rev. D, 71h, 3502

Kohri K., 2001, Phys., Rev. D, 64d, 3515

Kuhlen M., Madau P., Montgomeri R., 2006, ApJ, 637L, 1

Kuzmin, V.A., & Rubakov, V.A., 1998, Phys. Atom. Nucl., 61, 1028

Liszt H., 2001, A&A, 371, 698

Loeb A. & Zaldarriaga M., 2004, Phys. Rev. Lett. 92, 211301

Madau P., Haardt F., Rees M.J., 1999, ApJ, 514, 648

Madau P., Meiskin A., Rees M.J., 1997, ApJ, 475, 492

Mapelli M., Ferrara A., Pierpaoli E., 2006, MNRAS submitted, astro-ph/0603237

Miralda-Escudé J. & Rees M.J., 1994, MNRAS, 266, 343

Oh S.P., 2001, ApJ, 553, 499

Peebles P.J.E., Seager S., Hu W., 2000, ApJL, 539, L1

Pierpaoli E., Phys. Rev. Lett., 2004, 92, 031301

Ricotti M. & Ostriker J., 2004, MNRAS, 352, 547

Scherrer R. J., 1984, MNRAS, 210, 359

Sciama, D.W., 1982, MNRAS, 198, 1

Scott D., Rees M.J., Sciama D., 1991, A&A, 250, 295

Seager S., Sasselov D.D., Scott D., 1999, ApJ, 523L, 1

Sethi S., 2005, MNRAS, 363, 818

Shapiro P.R. & Giroux M.L., 1987, ApJL, 321, L107

Shull J.M. & van Steenberg M.E. 1985, ApJ, 298, 268

Spergel D. N., Verde L., Peiris H.V. et al, 2003, ApJS, 148, 175

Spergel D. N., Bean R., Doré O. et al, 2006, astro-ph/0603449

Tegmark M., Silk J., Blanchard A., 1994, ApJ, 434, 395

Tozzi P., Madau P., Meiskin A., Rees M.J., 2000, ApJ, 528, 597

Tumlinson J., Venkatesan A., Shull J.M., 2004, ApJ, 612, 602

Vayner B.V., Shchekinov Yu.A. & Entel M.B., 1985, Ap, 23, 733

Wyithe J.S.B. & Loeb A. 2003, ApJL, 588, L69

Zaldarriaga M., Furlanetto S.R., Hernquist L., 2004, ApJ, 608, 622

Zaroubi S. & Silk J., 2005, MNRAS, 360, 64,